Accepted Manuscript

Influence Of Loading Rate, Alkali Fibre Treatment And Crystallinity On Fracture Toughness Of Random Short Hemp Fibre Reinforced Polylactide Bio-composites

Kim L. Pickering, Moyeenuddin A. Sawpan, Jeevan Jayaraman, Alan Fernyhough

PII: S1359-835X(11)00134-5
DOI: 10.1016/j.compositesa.2011.04.020
Reference: JCOMA 2877

To appear in: *Composites: Part A*

Received Date: 22 September 2010
Revised Date: 22 March 2011
Accepted Date: 26 April 2011

Please cite this article as: Pickering, K.L., Sawpan, M.A., Jayaraman, J., Fernyhough, A., Influence Of Loading Rate, Alkali Fibre Treatment And Crystallinity On Fracture Toughness Of Random Short Hemp Fibre Reinforced Polylactide Bio-composites, *Composites: Part A* (2011), doi: 10.1016/j.compositesa.2011.04.020

Influence Of Loading Rate, Alkali Fibre Treatment And Crystallinity On Fracture Toughness Of Random Short Hemp Fibre Reinforced Polylactide Bio-composites

Kim L. Pickering[a], Moyeenuddin A. Sawpan[b*], Jeevan Jayaraman[a] and Alan Fernyhough [c]

[a] *School of Engineering, University of Waikato, Hamilton, New Zealand*

[b] *Composite Materials Research, Pultron Composites Ltd, Gisborne, New Zealand*

[c] *Biomaterials Engineering, Biopolymer Network/SCION, Rotorua, New Zealand*

Abstract

Plane-strain fracture toughness (K_{Ic}) of random short hemp fibre reinforced polylactide (PLA) bio-composites was investigated along with the effect of loading rate, fibre treatment and PLA crystallinity. Fracture toughness testing was carried out at loading rates varying from 0.5 to 20 mm/min using single-edge-notched bending specimens with 0 to 30 wt% fibre. K_Q (trial K_{Ic}) of composites decreased as loading rate increased, until stabilising to give K_{Ic} values at a loading rate of 10 mm/min and higher. The reduction of crazing and stress whitening, as well as a more direct crack path observed in PLA samples combined with reduced plastic deformation observed in composites provided explanation for this reduction. K_{Ic} of composites was found to decrease with increased fibre content and fibre treatment with sodium hydroxide. Studies controlling the degree of PLA crystallinity by heat treatment or "annealing" showed that reduction of K_{Ic} can be attributed to increased crystallinity.

Key words: A. Polymer-matrix composites (PMCs); A. Fibres; B. Fracture toughness; D. Fractography

* Corresponding author.

E-mail: moyeen@pultron.com; Tel: +64 6 867 8582; Fax: +64 6 867 8542

1. Introduction

In recent years, bio-based composite materials have been the focus of academic and industrial research interest from the viewpoint of reducing impact on the natural environment [1]. Polylactide (PLA) is considered one of the most promising renewable resource based biopolymer matrices. This is because the physical and mechanical properties of PLA make it a good alternative to currently used commodity polymers such as polypropylene and poly(ethylene terepthlate) and it is readily fabricated to produce injection moulded parts, film, or fibres [2, 3].

For structural application, there is a need to better understand and describe the fracture behaviour of PLA. Fracture toughness of a given material is a function of testing speed and temperature [4] and so assessment of rate dependent fracture mechanisms is important for the designer in understanding mechanical performance of composites [5]. Reduction of fracture toughness with increased testing rate has been observed for polymers including PLA [5-7] and has been associated with the reduction of crazing and plastic blunting at the crack tip for higher loading rates corresponding to the reduction of energy dissipation. Although many research works have reported the influence of loading rate on fracture toughness of synthetic fibre reinforced composites [6-9], the

vast majority of these are based on continuous fibre composites, although increasingly brittle behaviour has been reported with short glass fibres at higher loading rates. Interfacial strength and mechanical properties such as tensile, flexural, impact, creep and fatigue of natural fibre reinforced bio-composites have been reported by other researchers [10-14]. However, there is no literature on the effects of loading rate on fracture toughness of short natural fibre reinforced bio-composites, which have high potential in load bearing engineering applications.

When natural fibres are used as a reinforcing material in semicrystalline polymer matrices such as PLA, they can act as nucleating sites for crystal growth and commonly a transcrystalline layer grows from the crystalline cellulose surfaces [1, 15, 16] which is likely to influence fracture. Previous studies [17, 18] demonstrated that reinforcing hemp fibre increases the tensile strength, Young's modulus, impact strength and flexural modulus of PLA bio-composites which is a good indication of compatibility of hemp fibre with PLA. The objective of this work was to investigate fracture toughness of random short hemp fibre reinforced PLA bio-composites over a range of loading rates, fibre contents, and different levels of matrix crystallinity along with the effect of fibre treatment to elucidate important factors influencing this parameter.

2. Experimental

2.1. Materials

NatureWorks® PLA (polylactide) polymer 4042D, from NatureWorks LLC, USA, was used as a matrix. This was provided in a pellet form with a density of 1.25 g/cc. Retted hemp bast fibre was supplied by Hemcore, UK. The average length and diameter of the fibre were 65mm and 31.5μm, respectively.

2.2. Fibre Treatment

Fibres were washed with hot water (50°C) to remove dirt and impurities, dried and then soaked in 5 wt% sodium hydroxide (NaOH) solution at ambient temperature, maintaining a fibre:solution ratio of 20:1 (by weight). The fibres were immersed in the solution for 30 min. After treatment, fibres were copiously washed with water and subsequently neutralised with 1 wt% acetic acid solution. The treated fibres were then dried in an oven at 80°C for 48 h. The average diameter of the fibres was decreased to 25.8μm after treatment due to the removal of external impurities (e.g. wax).

2.3. Cellulose crystallinity index

Approximately 15 mg of fibres were cut and pressed into a disk using a cylindrical steel mould with an applied pressure of 10 MPa in laboratory hydraulic press. Cellulose crystallinity index (I_{XRD}) was calculated by means of the Segal equation as follows [19, 20]:

$$I_{XRD}\,(\%) = \frac{I_{002} - I_{amp}}{I_{002}} * 100 \qquad (1)$$

where I_{002} is the maximum intensity of the 002 lattice diffraction plane at an angle 2θ of between 22° and 23° ($22^{o} \leq 2\theta \leq 23^{o}$) and I_{amp} is the intensity diffraction at an angle 2θ close to 18° representing amorphous materials in cellulosic fibres.

2.4. Interfacial strength measurement

For pull-out specimen preparation, a hole of 6 mm diameter was made in a silicone rubber mould (18mm x 24mm x 3 mm) positioned relatively central and near to one of the two longest sides using a punch (see Fig. 1). A slot was cut to a depth of 2.5 mm to give a channel from the outer wall of the mould to the punched hole. The mould was flexed to open the cut to allow the introduction of a fibre and then released to grip the

fibre. The desired embedded length was obtained by drawing the fibre through the cut under optical light microscope. Fibre diameters were measured using an optical microscope with a calibrated eye-piece. Then the mould was placed on a piece of polytetrafluoroethylene (PTFE) sheet on a glass plate, and two small pieces from a PLA pellet were placed into the mould cavity. This was then placed in a pre-heated oven (180^{o}C) for 5 min and then allowed to cool in air at room temperature. Samples were prepared with a range of embedded lengths from 0.25 mm to 2 mm with a free-fibre length of approximately 5 mm. The free-fibre end was glued to a piece of cardboard. Pull-out testing was performed on an Instron 4204 Universal Testing machine. The sample was gripped at the upper cross-head and the paper cardboard was gripped by the stationary bottom part. The force was measured with an accuracy of ± 0.1 mN. Interfacial strength (τ_{po}) was calculated using the following equation [10, 21]:

$$\tau_{po} = \frac{F_{\max}}{\pi d l_e} \quad (2)$$

where F_{max} is the maximum load, d is the fibre diameter and l_e is the embedded length.

2.5. Single Fibre Testing

Single fibre tensile strength of hemp fibres was measured according to the ASTM D3379-75 Standard Test Method for Tensile Strength and Young's Modulus for High-Modulus Single Filament Materials [22]. Specimens were prepared by separating fibre bundles by hand, and then attaching single fibres to cardboard mounting-cards using polyvinyl acetate glue with 10 mm holes punched into them to give a gauge length of 10 mm. The mounted fibres were then placed in the grips of an Instron 4204 tensile testing machine, and a hot-wire cutter was used to cut the supporting sides of the mounting cards.

2.6. Composite Processing

Hemp fibres (average length 4.9 mm) were initially washed with hot water and the fibre and PLA were dried in an oven at 80°C overnight. PLA/hemp fibre composites were compounded (10, 15, 20 and 30 wt% fibre) in a ThermoPrism TSE-16-TC twin screw extruder. The extruder barrel consisted of 5 heating zones, which were set at 110°C, 130°C, 180°C, 190°C, and 185°C from feed zone to die exit. The screw diameter was 15.6mm and the co-rotating screws were operated at 100 rpm. The extruded composite material was pelletised and dried at 80°C for 24 h and then injection moulded using a BOY15-S injection moulding machine. The feeding, compression and metering sections of the injection moulding machine were set at 155 °C, 180 °C and 190°C, respectively. The injection screw speed was set at 160 rpm. Fibre length distribution and fibre diameter of the composites are available elsewhere [23].

2.7. Composite Annealing

Alkali treated fibre composite samples were heat treated or "annealed" at 70°C and 100°C (above glass transition temperature of PLA (i.e. 57.8°C)) for 3, 8 and 24 h in an oven.

2.8. Differential scanning calorimetry (DSC)

DSC scans were carried out at a scan rate of 10°C/min from room temperature to 200°C in the presence of air using samples of approximately 10 mg to assess the influence of fibre content and fibre treatment on the crystallinity of PLA. The crystallinity (X_{DSC}) of PLA was calculated using the following equation [16]:

$$X_{DSC}(\%) = \frac{\Delta H_f - \Delta H_{cc}}{\Delta H_f^o} \times \frac{100}{w} \quad (3)$$

where $\Delta H^o_f = 93$ J/g for 100% crystalline PLA, ΔH_f is the enthalpy of melting, ΔH_{cc} is the cold crystallisation enthalpy and w is the weight fraction of PLA in the composite.

2.9. Fracture toughness testing

Fracture toughness testing was carried out using single-edge-notched bend (SENB) specimens according to the ASTM D 5045-99 Standard Test Methods for Plane-Strain Fracture Toughness and Strain Energy Release Rate of Plastic Materials. The length (L), span length (S), width (W) and thickness (B) of the specimens were 126, 56, 12.7 (± 0.03) and 3.5 (± 0.03) mm respectively, which satisfies the condition 2B<W<4B as specified in the standard. The initial crack length (a) was 6.35 mm (± 0.005). The loading speed was varied from 0.5 mm/min to 20 mm/min and the notch root of the specimens was sharpened using a razor blade before testing. Four replicate specimens were tested. Mode I plane-strain fracture toughness (K_{Ic}) of single-edge-notch-bending (SENB) specimens was calculated with the following relationships [4]:

$$K_Q = \left(\frac{P_Q}{BW^{1/2}} \right) f(x) \tag{4}$$

where K_Q, P_Q, B and W are trial K_{Ic}, maximum load, specimen thickness and width, respectively,

and $$f(x) = 6x^{1/2} \frac{\left[1.99 - x(1-x)(2.15 - 3.93x + 2.7x^2)\right]}{(1+2x)(1-x)^{3/2}} \tag{5}$$

such that $x = a/W$, where a is the initial crack length. In order for K_Q to be considered the plane-strain fracture toughness, K_{Ic}, the following size criterion must be satisfied:

$$B, a, (W-a) > 2.5(K_Q/\sigma_t)^2 \tag{6}$$

where σ_t is the tensile strength obtained from tensile testing performed based on ASTM D 638 Test Method for Tensile Properties of Plastics [24] with loading rate and

temperature the same as for fracture toughness testing. Four samples were tested for each batch of samples.

2.10. Light microscopy

To allow for visual inspection of crystallinity, single fibre samples were prepared by embedding a hemp fibre in molten PLA between two slides and squeezing the slides together. Then the sample was allowed to cool down to room temperature to allow solidification of the PLA then inspected. Fracture surfaces were also inspected using an Olympus BX60F5 optical light microscope and a WILD M3B stereo microscope. Micrographs were obtained using a Nikon camera (Digital Sight DS-U1).

3. Results and Discussion

3.1 Effect of Fibre Treatment on Single Fibre Properties and Interfacial Shear Strength

Crystallinity index of fibres was found to increase compared with untreated fibres (91.6% compared with 87.9%). This is likely to be due to removal of amorphous components allowing better alignment of cellulose chains as observed elsewhere [25]. This correlated with an increase in average fibre tensile strength (from 577 to 598 MPa), although this increase was found to not be statistically significant. Interfacial shear strength (IFSS) of the PLA/hemp fibre samples as a function of fibre embedded length is depicted in Fig. 2. The non-linear relationship between these two parameters is indicative of a brittle-like interface fracture as reported in the literature [26] such that catastrophic failure occurs once a critical crack length is achieved. Average interfacial shear strengths increased from 5.55 MPa for untreated fibre to 11.41 MPa for alkali treated fibres, which is likely to be due to the removal of non-cellulosic material allowing stronger bonding between PLA and cellulose at the interface.

3.2. Effect of Fibre Content and Fibre Treatment on PLA Crystallinity

PLA crystallinity in composites was found to increase with fibre content, which is in agreement with findings in the literature [16], as well as with fibre treatment as shown in Fig. 3, suggesting that the fibre acts as a nucleating agent which is more effective when more crystalline cellulose is exposed. Fig. 4 shows a single untreated fibre composite sample exhibiting crystallinity including spherulites in the PLA as well as transcrystallinity at the fibre/matrix interface further supporting that the fibre acts as a nucleating agent. The amount of transcrystallinity was observed to increase with fibre treatment (see Fig. 5).

3.3. Fracture Toughness Testing

Load-displacement behaviour

Typical load-displacement graphs for PLA and composites under various loading rates are depicted in Fig. 6. It may be observed that these showed initially linear deformation, followed by an amount of non-linear deformation prior to the attainment of maximum load. Once the maximum load was attained, the recorded load diminished gradually which was most probably a result of cracking along with limited plastic deformation. It can be easily seen that the curves became steeper with increased fibre content. This behaviour was expected because the Young's modulus of the hemp fibre is superior to that of PLA. It is also evident that the area under the curves decreased with increased loading rate. This observation is attributed to decreased plastic deformation at higher loading rates.

As can be seen clearly in Fig. 7, if a line (AC) is drawn with a gradient of 5% less than that of the tangent (AB) to the original loading line, the recorded maximum load ($P_{\max}$), lies between these two lines, which thus meets the requirement of the standard [4] for

allowance of $P_{\max}$ to be used as P_Q for the calculations of K_Q (see Eq. 4). This form of load-displacement behaviour was observed for all the samples tested.

Effect of loading rate and fibre content

The tensile strength of PLA and composites for two different loading rates is summarised in Table 1. The tensile strength was found to increase with fibre content and was higher at higher testing speeds which would be expected due to less time for thermal fluctuations within the material to assist with molecular flow. Further details of tensile properties including stress-strain curves and Young's modulus are given elsewhere [17]. Fig. 8 illustrates K_Q of PLA and composites as a function of loading rate. It can be seen that K_Q for all fibre contents decreased with increased loading rate up to 10mm/min above which it stabilised at a constant value. It was found (using Eq. 6) that at a loading rate of 5 mm/min, K_Q of the matrix and composites did not satisfy plane strain conditions. On the other hand, K_Q at a loading speed of 10 mm/min was found to fulfil the required criteria given in Eq. 6 and therefore be equivalent to K_{Ic}. Since the magnitude of K_Q from 10 mm/min to higher loading rates was approximately constant, and given the general expectation of increased yield strength with increased loading rate, it is likely that the criterion of Eq. 6 was also met for the higher loading rates above 10 mm/min.

Also from Fig. 8, it is evident that K_Q of the PLA/hemp composites decreased with increased fibre content. One possible influence is the stress concentration due to the presence of fibres. However, research elsewhere on PLA [27], has shown the reduction of fracture toughness with increased crystallinity which could be a factor here. Fig. 9

presents DSC traces from which PLA crystallinity values were calculated (as well as depicting the glass transition point and cold crystallisation and melting peaks) and Fig. 10 shows the relationship of composite K_{Ic} and PLA crystallinity obtained at different fibre contents, which demonstrates a convincing trend of decreasing K_{Ic} with increased crystallinity.

Fractography of PLA and composites

Light micrographs of cracks (side view) of the PLA samples tested under different loading rates are shown in Fig. 11. As can be seen, extensive crazing was generated in the crack-tip region for samples tested at lower loading rates (1 and 5 mm/min), but not so apparent at higher loading rates (including 10 mm/min).

Typical fracture surfaces of PLA investigated for a range of loading rates are presented in Fig. 12. The fracture surfaces showed two distinct zones, namely a smooth zone suggesting brittle-like fracture next to the initial starter notch and a stress-whitened zone associated with crazing. A reduction in the stress-whitened region and increase in size of the smooth brittle-like region further supported that at higher loading rates crack propagation involved less crazing leading to lower K_Q values.

Typical crack paths of PLA/hemp composites (side view) tested at 5 mm/min and 10mm/min are presented in Figs. 13 and 14, respectively. As can be seen, cracks were initiated from the tip of the pre-existing crack, but did not propagate directly across the sample and appear to have been influenced by the presence of fibres such that increased fibre volume fraction resulted in a more irregular crack path. Within the composites tested at 5 mm/min (Fig. 13), evidence of localised matrix tearing is present suggesting

limited plastic deformation. A closer examination of the crack propagation path indicates that the two fracture surfaces were not completely separated, but rather connected by the deformed matrix. This behaviour was commonly observed for all the samples at lower loading rates, irrespective of the amount of fibre content. There was a significant reduction in the plastic flow and/or matrix tearing when the samples were tested at 10 mm/min (Fig. 14) which could explain the reduction of K_Q at higher loading rates. In contrast to lower loading rates, the two fracture surfaces were completely separated ahead of the starter crack.

Effect of Fibre Treatment

Fig. 15 presents a comparison of K_{Ic} values obtained at a rate of 10mm/min for untreated and treated fibre composites at different fibre contents. These composites were made from a more recently procured batch of fibre than earlier experiments, which explains the slight differences for untreated fibres values compared to those in Fig. 8. K_{Ic} values for treated fibre composites followed the same trend of reduction with increased fibre content as for untreated fibre composites, but were lower. This could have been due to improved interfacial bonding leading to easier crack propagation, although it has been seen that crystallinity increases with fibre treatment and again as for increased fibre content could be playing a role in reduced K_{Ic}.

Effect of annealing on PLA Crystallinity

Fig. 16 shows the effect of heat treating or "annealing" treated fibre composites for different times at different temperatures on PLA crystallinity conducted in order to isolate its effect on K_{Ic}. The crystallinity for the control PLA samples was around 3%. This increased slightly with the presence of fibre. Only limited increase in crystallinity was observed for 3 h at 70°C. On increased duration of annealing at 70°C, PLA only

samples were relatively unaffected whereas composites were seen to undergo a significant increase in crystallinity, supporting that hemp fibre acts as a nucleating agent. Further increases were seen when annealing at 100°C for 24 h (close to the cold crystallinity peak temperature for PLA) was carried out, where crystallinity reached up to approximately 35% for PLA and up to 51% for composites of 15 wt% fibre. The effect of crystallinity on K_{Ic} is presented in Fig. 17. The trend lines show a reduction of K_{Ic} for PLA and composites as crystallinity increased, although there is not a clear trend between the two different fibre contents.

4. Conclusions

In this work, K_Q of random short hemp fibre reinforced PLA bio-composites was found to decrease with increased loading rate until plane strain conditions were met at 10mm/min and above. K_{Ic} was found to decrease with increased fibre content and fibre treatment coinciding with an increase in crystallinity. Heat treatments conducted to isolate the effect of crystallinity showed that K_{Ic} is reduced by increased crystallinity, suggesting that transcrystallinity within the composites is having a large influence on the fracture behaviour of composites and may serve as an easy path for crack propagation. However, increased stress concentration with increased fibre content and increased interfacial strength with treatment may also be contributing to reduction of K_{Ic} for composites. It is concluded that it is possible to improve fracture toughness of this type of composite by controlling crystallinity during composite production.

Acknowledgement

Financial support from Biopolymer Network Ltd, New Zealand is gratefully acknowledged.

References

[1] R. Masirek, Z. Kulinski, D. Chionna, E. Piorkowska, and M. Pracella, Composites of poly(L-lactide) with hemp fibers: Morphology and thermal and mechanical properties, Journal of Applied Polymer Science 105 (2007) 255-268.

[2] D. Plackett, T. L. Andersen, W. B. Pedersen, and L. Nielsen, Biodegradable composites based on L-polylactide and jute fibres, Composites Science and Technology 63 (2003) 1287-1296.

[3] S. Serizawa, K. Inoue, and M. Iji, Kenaf-fiber-reinforced poly(lactic acid) used for electronic products, Journal of Applied Polymer Science 100 (2006) 618-624.

[4] Standard Test Methods for Plane-Strain Fracture Toughness and Strain Energy Release Rate of Plastic Materials, ASTM D 5045 (1999).

[5] R. Gensler, C. J. G. Plummer, C. Grein, and H. H. Kaysch, Influence of the loading rate on the fracture resistance of isotactic polypropylene and impact modified isotactic polypropylene, Polymer 41 (2000) 3809-3819.

[6] G. C. Jacob, J. M. Starbuck, J. F. Fellers, S. Simunovic, and R. G. Boeman, Fracture toughness in random-chopped fiber-reinforced composites and their strain rate dependence, Journal of Applied Polymer Science 100 (2006) 695-701.

[7] J. W. Gillespie, L. A. Carlsson, and A. J. Smiley, Rate-dependent mode I interlaminar crack growth mechanisms in graphite/epoxy and graphite/PEEK, Composites Science and Technology 28 (1987) 1-15.

[8] I. Levay, G. B. Lenkey, L. Toth, and Z. Major, The effect of the testing conditions on the fracture mechanics characteristics of short glass fibre reinforced polyamide, Journal of Materials Processing Technology 133 (2003) 143-148.

[9] J. Karger-Kocsis, and K. Friedrich, Temperature and strain-rate effects on the fracture toughness of poly(ether ether ketone) and its short glass-fibre reinforced composite, Polymer 27 (1986) 1753-1760.

[10] S. Wong, R. A. Shanks, and A. Hodzic, Effect of additives on the interfacial strength of poly(L-lactic acid) and poly(3-hydroxy butyric acid)-flax fibre composites, Composites Science and Technology 67 (2007) 2478-2484.

[11] R. Tokoro, D. M. Vu, K. Okubo, T. Tanaka, T. Fujii, and T. Fujiura, How to improve mechanical properties of polylactic acid with bamboo fibers, Journal of Materials Science 43 (2008) 775-787.

[12] B. Bax, and J. Mussig, Impact and tensile properties of PLA/Cordenka and PLA/flax composites, Composites Science and Technology 68 (2008) 1601-1607.

[13] S. Wong, and R. A. Shanks, Creep behaviour of biopolymers and modified flax fibre composites, Composite Interfaces 15 (2008) 131-145.

[14] S. Wong, R. A. Shanks, and A. Hodzic, Mechanical behavior and fracture toughness of poly(L-lactic acid)-natural fiber composites modified with hyperbranched polymers, Macromolecular Materials and Engineering 289 (2004) 447.

[15] A. P. Mathew, K. Oksman, and M. Sain, The effect of morphology and chemical characteristics of cellulose reinforcements on the crystallinity of polylactic acid, Journal of Applied Polymer Science 101 (2006) 300-310.

[16] S. Pilla, S. Gong, E. O'Neill, R. M. Rowell, and A. M. Krzysik, Polylactide-pine wood flour composites, Polymer Engineering and Science 48 (2008) 578-587.

[17] M. A. Sawpan, K. L. Pickering, and A. Fernyhough, Improvement of mechanical performance of industrial hemp fibre reinforced polylactide biocomposites, Composites Part A: Applied Science and Manufacturing 42 (2011) 310-319.

[18] M. A. Sawpan, K. L. Pickering, and A. Fernyhough, Characterisation of hemp fibre reinforced Poly(Lactic Acid) composites, International Journal Materials and Product Technology 36 (2009) 229-240.

[19] L. Y. Mwaikambo, and M. P. Ansell, Chemical modification of hemp, sisal, jute, and kapok fibers by alkalization, Journal of Applied Polymer Science 84 (2002) 2222-2234.

[20] M. Le Troedec, D. Sedan, C. Peyratout, J. P. Bonnet, A. Smith, R. Guinebretiere, V. Gloaguen, and P. Krausz, Influence of various chemical treatments on the composition and structure of hemp fibres, Composites Part A: Applied Science and Manufacturing 39 (2008) 514-522.

[21] S. Zhandarov, and E. Mader, Characterization of fiber/matrix interface strength: applicability of different tests, approaches and parameters, Composites Science and Technology 65 (2005) 149-160.

[22] Standard Test Method for Tensile Strength and Young's Modulus for High-Modulus Single-Filament Materials, ASTM D 3379 (1989).

[23] M. A. Sawpan, Mechanical Performance of Industrial Hemp Fibre Reinforced Polylactide and Unsaturated Polyester Composites, PhD Thesis, The University of Waikato (2009).

[24] Standard Test Method for Tensile Properties of Plastics, ASTM D 638 (2003).

[25] K. L. Pickering, G. W. Beckermann, S. N. Alam, and N. J. Foreman, Optimising industrial hemp fibre for composites, Composites Part A (Applied Science and Manufacturing) 38 (2007) 461-468.

[26] A. Stamboulis, C. Baillie, and E. Schulz, Interfacial characterisation of flax fibre-thermoplastic polymer composites by the pull-out test, Angewandte Makromolekulare Chemie 272 (1999) 117-120.

[27] M. Todo, P. Sang Dae, K. Arakawa, and M. Koganemaru, Effect of crystallinity and loading-rate on mode I fracture behavior of poly(lactic acid), Polymer 47 (2006) 1357-1363.

Figure Captions

Fig. 1. Specimen preparation schematic for pull-out testing.

Fig. 2. Interfacial shear strength (IFSS) versus embedded length for untreated and alkali treated fibre in PLA.

Fig. 3. PLA crystallinity versus fibre content for untreated and alkali treated fibre composites at different fibre contents.

Fig. 4. Light micrograph of PLA crystallinity in PLA/hemp single fibre composite (scale bar = 100 μm).

Fig. 5. Light micrographs showing transcrystalline layer of PLA with (a) untreated and (b) treated hemp fibre surfaces (scale bar = 50 μm).

Fig. 6. Typical load-displacement curves of PLA and composites (PLA/untreated fibre) at (a) 5 mm/min, and (b) 10 mm/min.

Fig. 7. Measurement method of P_Q from a load-displacement curve.

Fig. 8. K_Q as a function of loading rate at different fibre contents.

Fig. 9. DSC traces for PLA and composites.

Fig. 10. Relationship between K_{Ic} and crystallinity for PLA and composites of different fibre contents.

Fig. 11. Light micrographs (side view) of crazing formed in PLA during fracture toughness testing at different loading rates (scale bar = 500μm).

Fig. 12. Light micrographs of PLA fracture surfaces tested at loading rates of: (a) 1 mm/min, (b) 5 mm/min, and (c) 10 mm/min.

Fig. 13. Light micrographs showing fracture behaviour of PLA/hemp composites (side view) tested at a loading speed of 5 mm/min at: (a) low magnification and (b) high magnification as a function of fibre content.

Fig. 14. Light micrographs showing fracture behaviour of PLA/hemp composites (side view) tested at a loading speed of 10 mm/min at: (a) low magnification and (b) at high magnification as a function of fibre content.

Fig. 15. K_{Ic} versus fibre content comparing untreated and alkali treated fibre composites.

Fig. 16. PLA crystallinity for different annealing treatments

Fig. 17. K_{Ic} versus crystallinity isolated from fibre content for alkali treated fibre composites

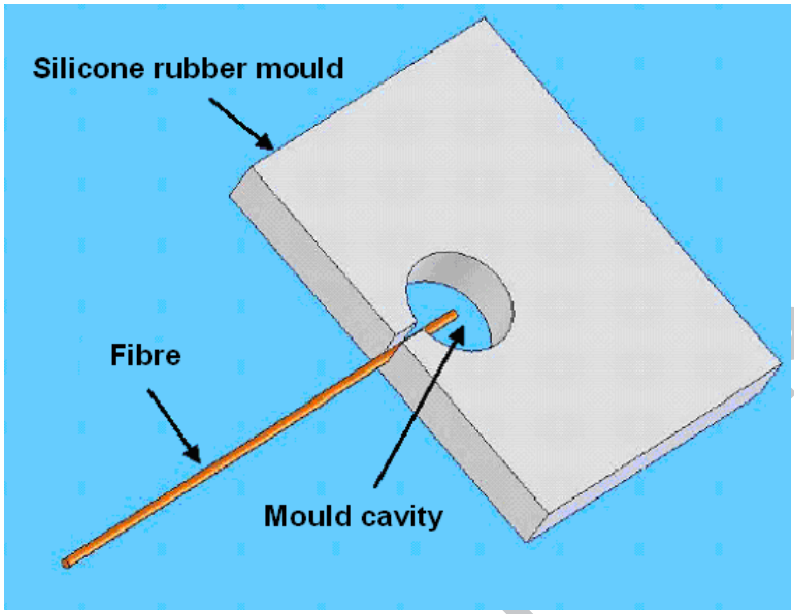

Fig. 1.

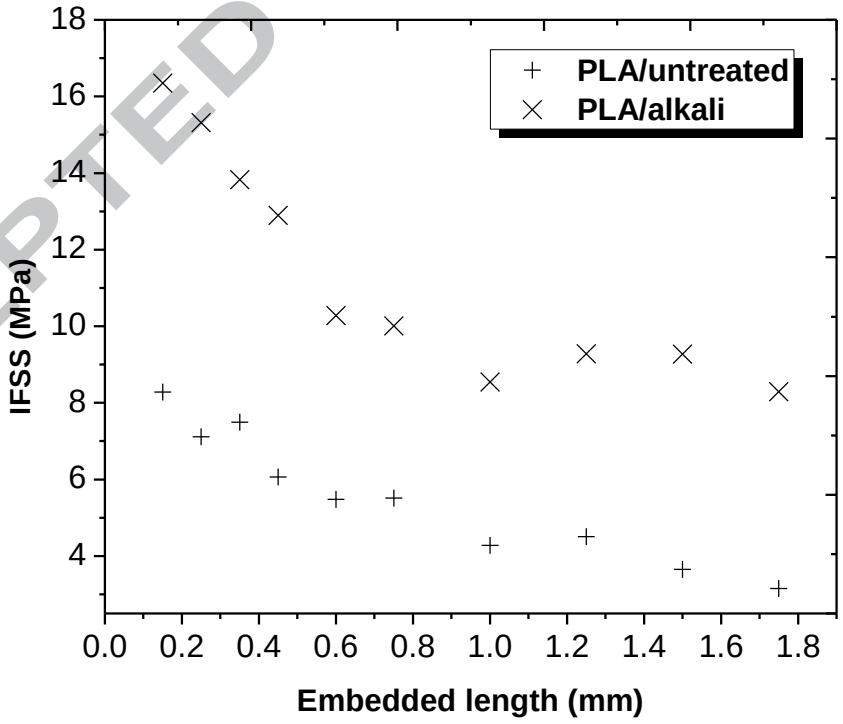

Fig. 2.

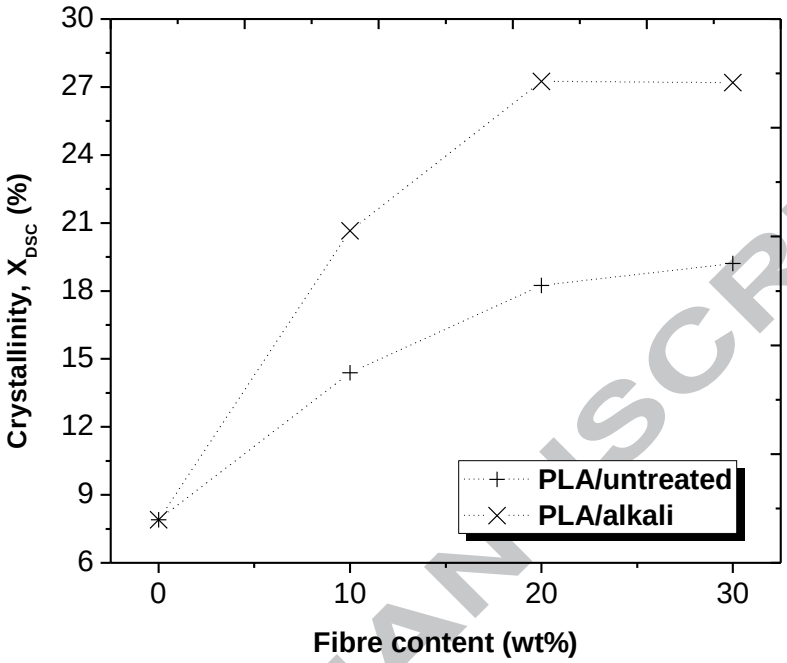

Fig. 3.

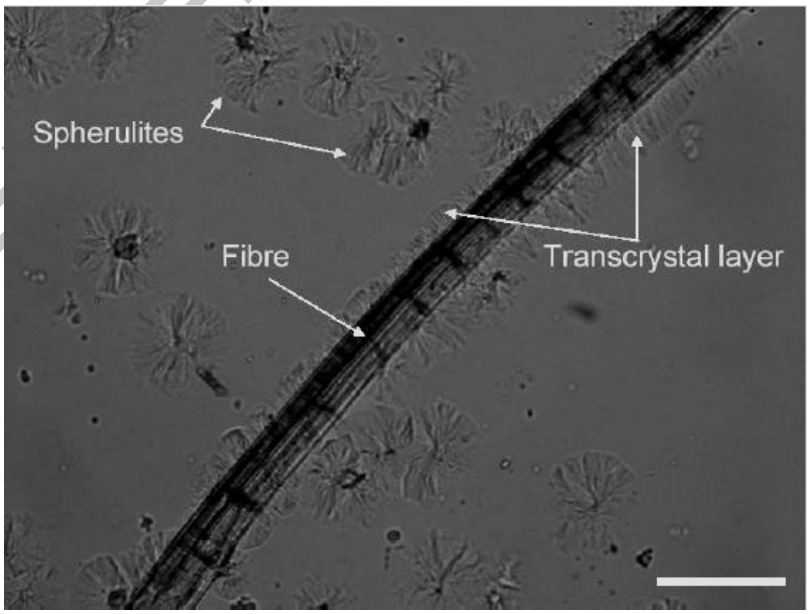

Fig. 4.

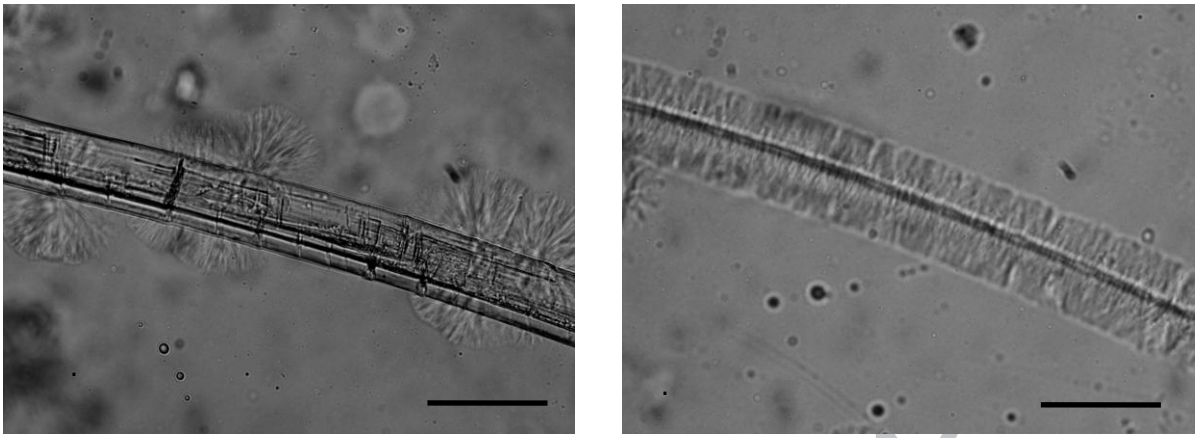

(a) (b)

Fig. 5.

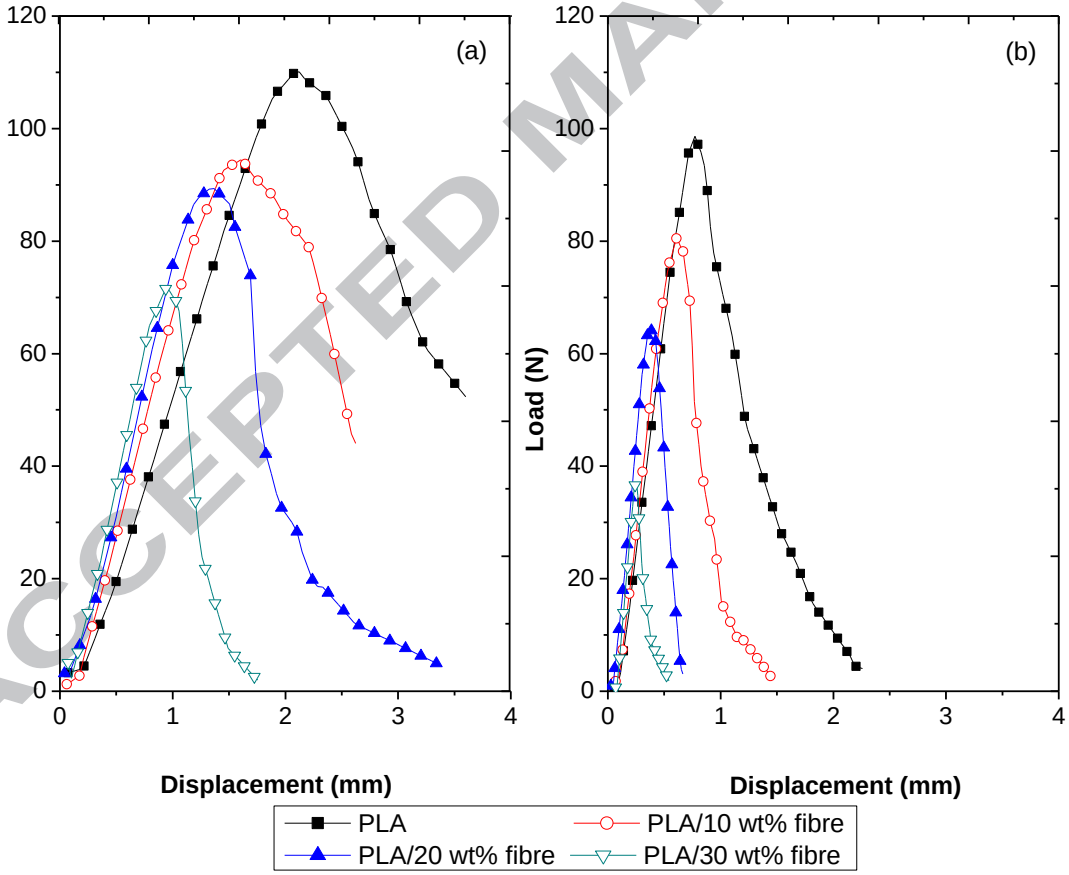

Fig. 6.

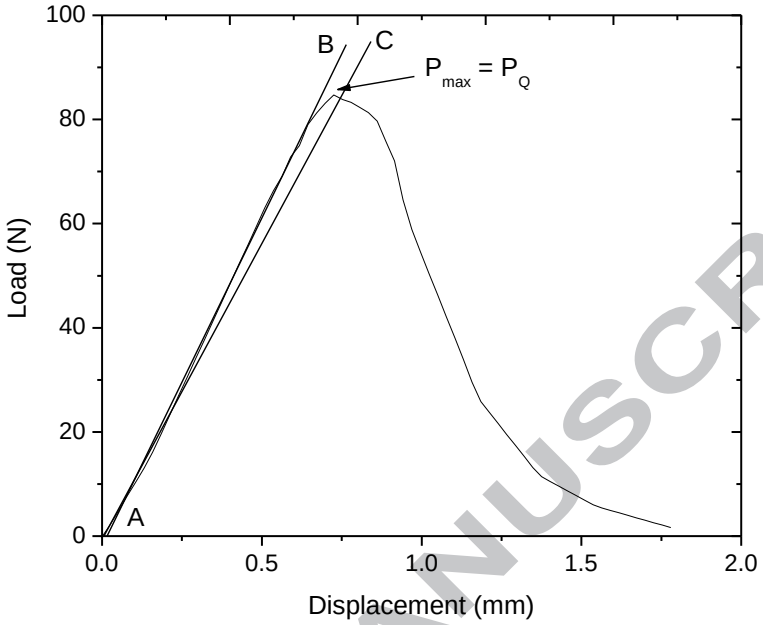

Fig. 7.

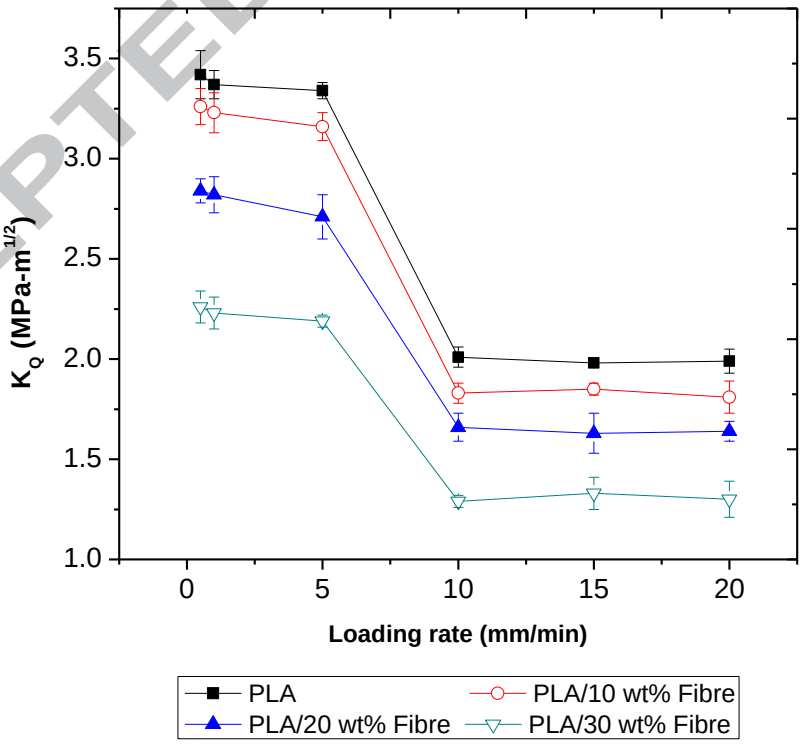

Fig. 8.

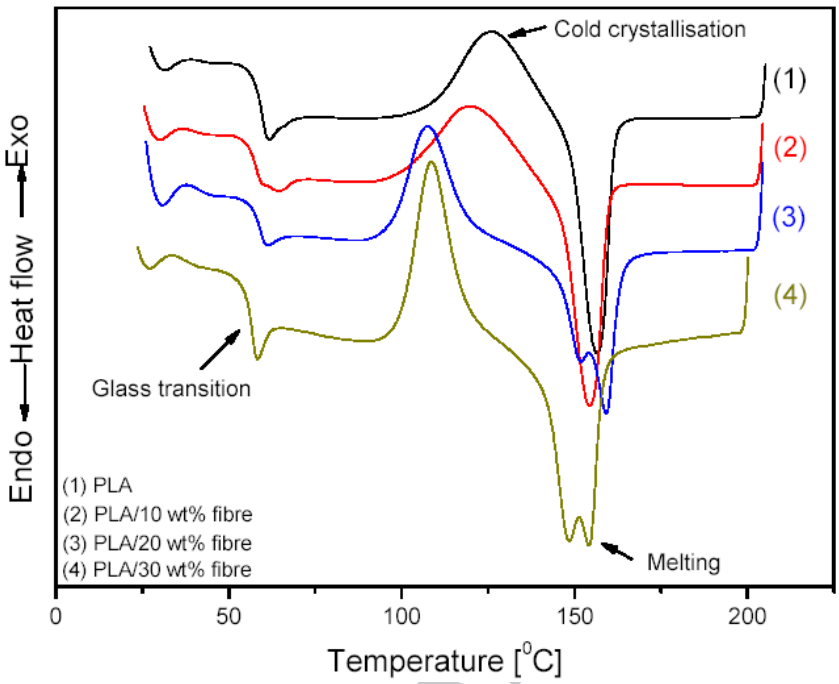

Fig. 9.

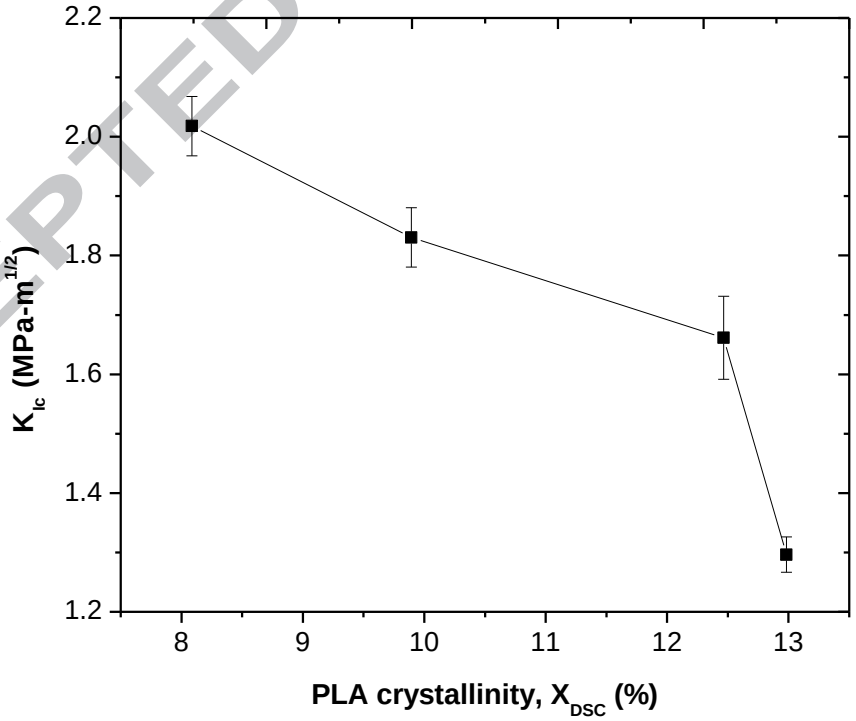

Fig. 10.

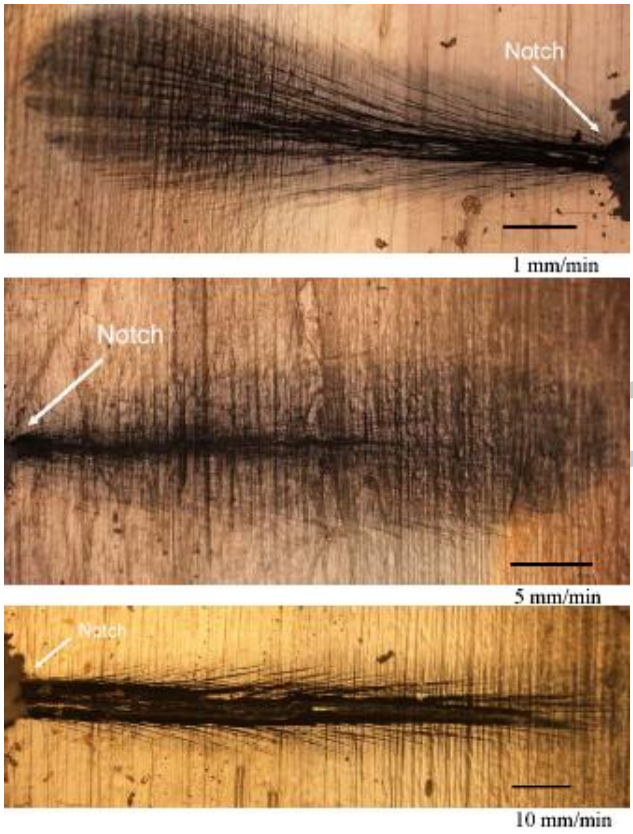
Notch
1 mm/min
Notch
5 mm/min
Notch
10 mm/min

Fig. 11.

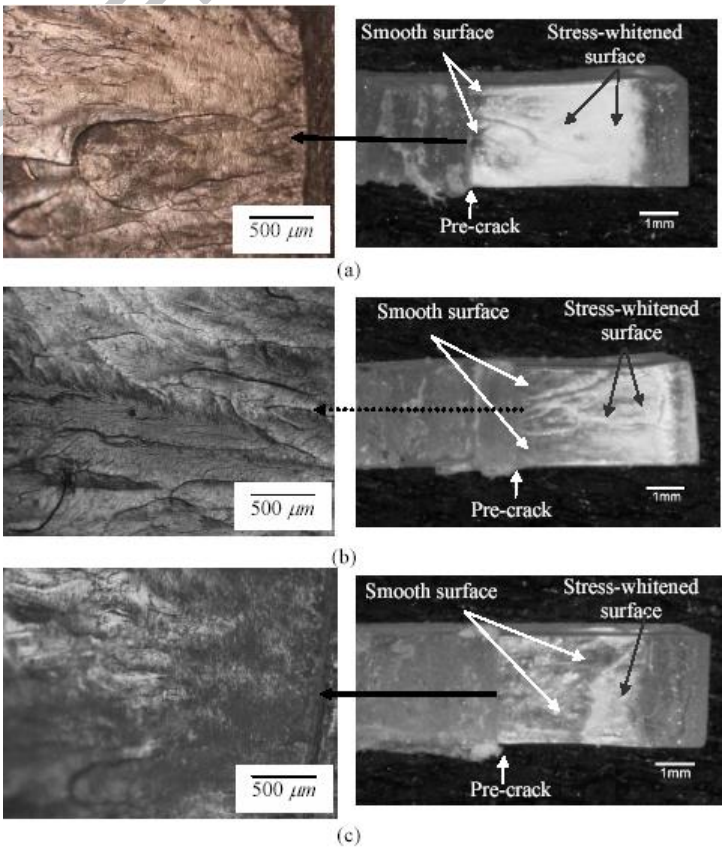
Smooth surface
Stress-whitened surface
Pre-crack
1mm
500 μm
(a)
Smooth surface
Stress-whitened surface
Pre-crack
1mm
500 μm
(b)
Smooth surface
Stress-whitened surface
Pre-crack
1mm
500 μm
(c)

Fig. 12.

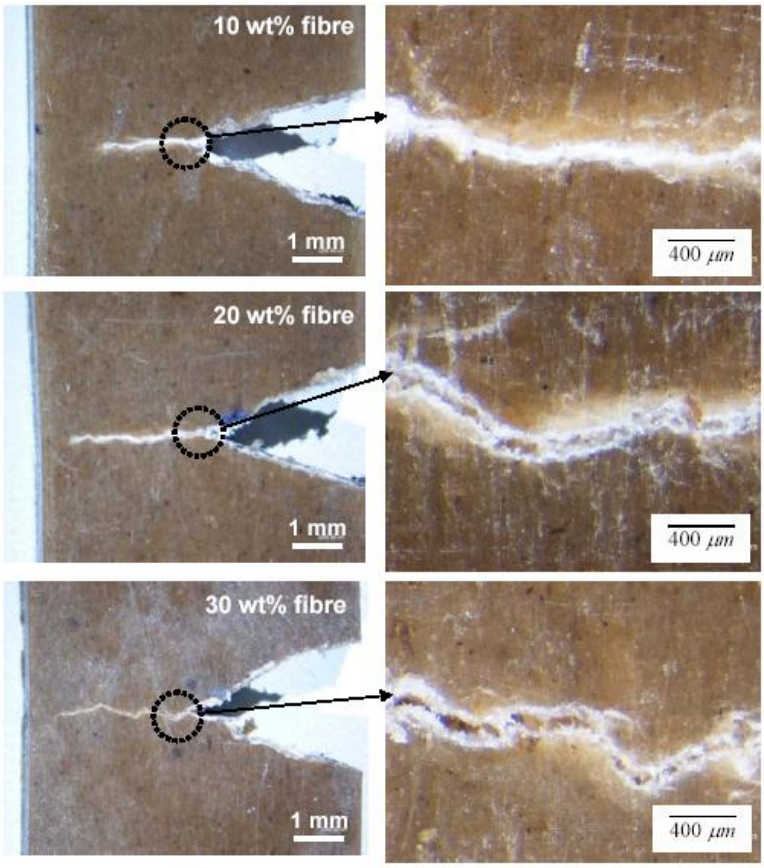

Fig. 13.

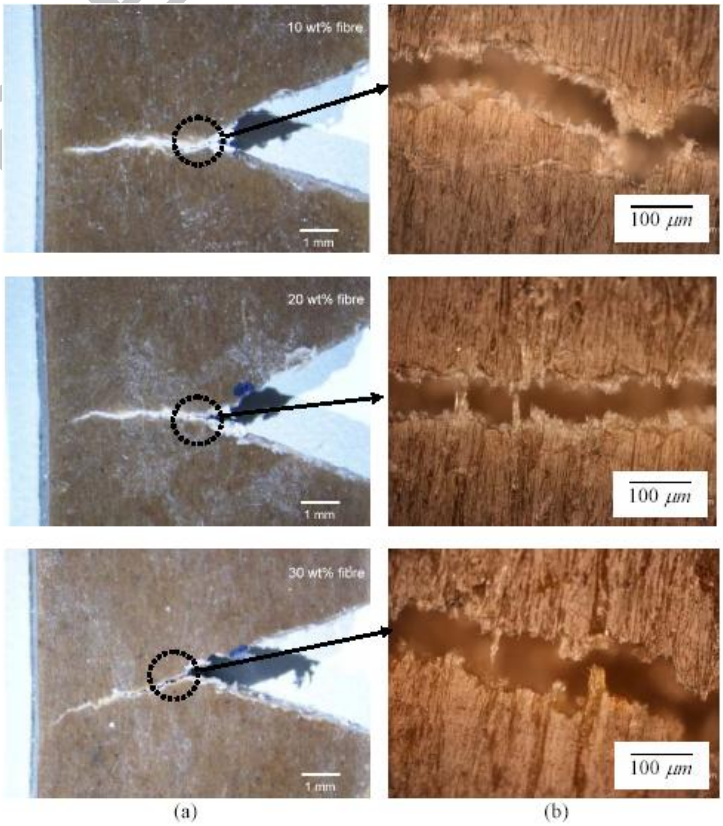

Fig. 14.

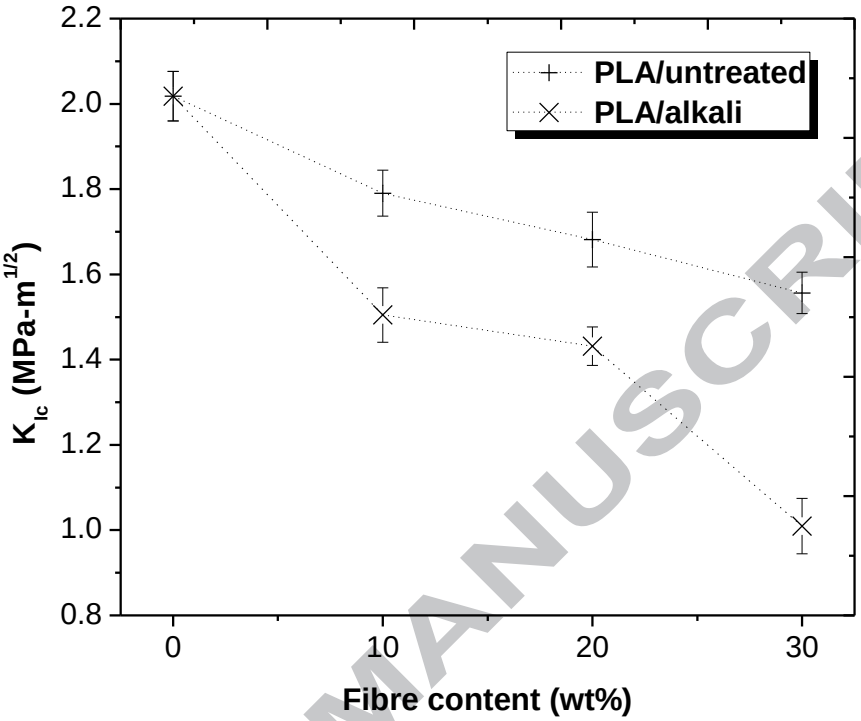

Fig. 15.

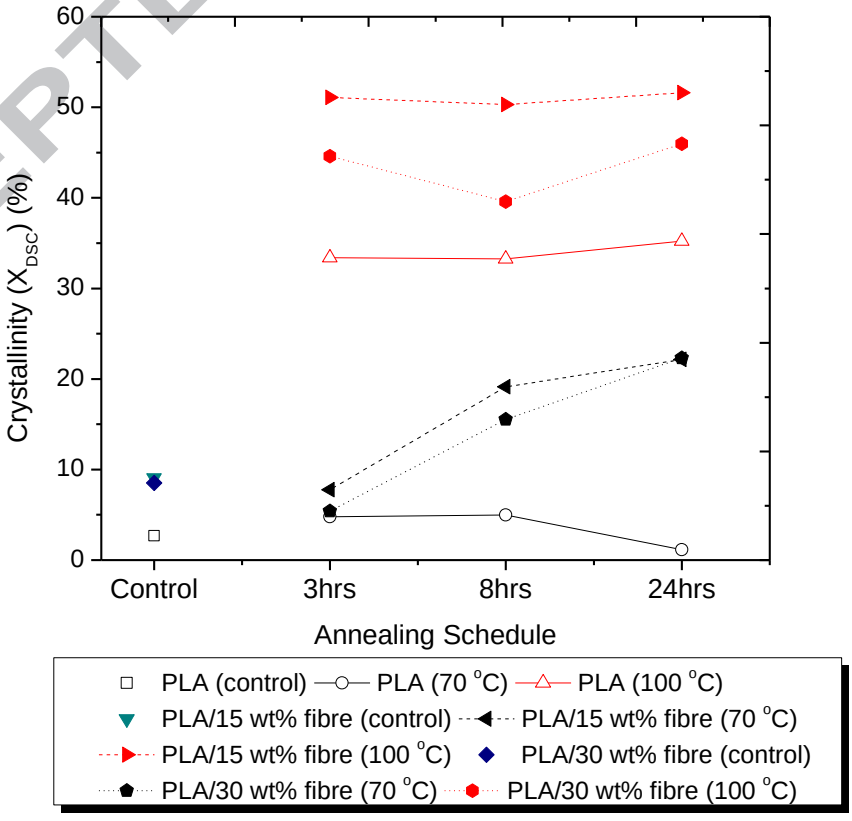

Fig. 16.

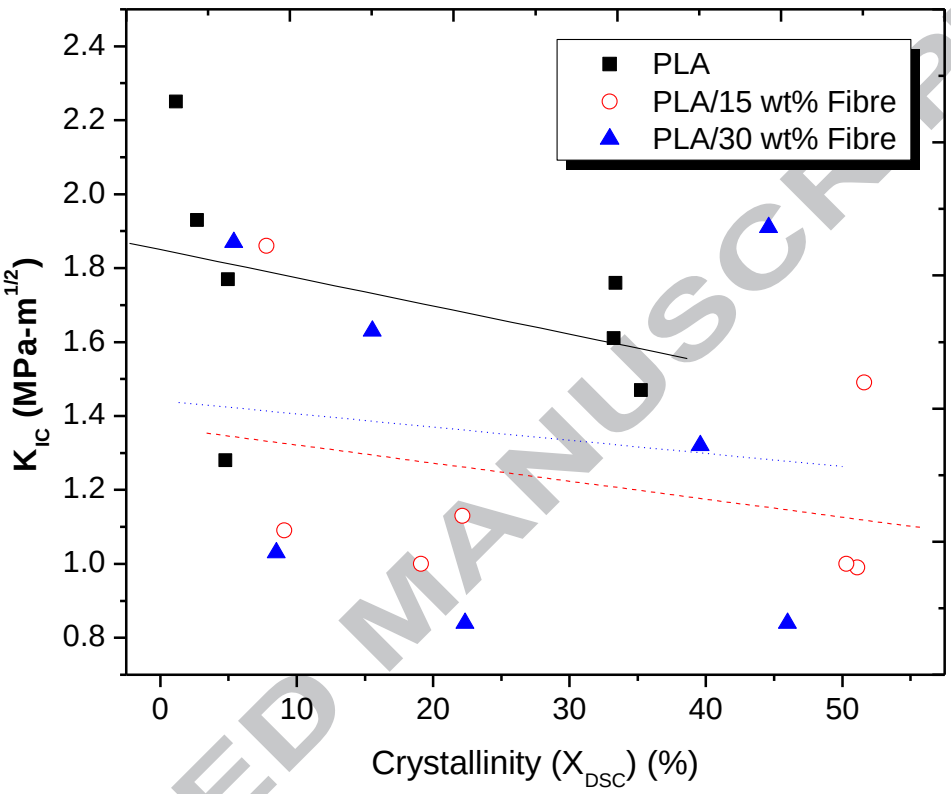

Fig. 17.

Table 1
Tensile strength of PLA and composites at two different testing speeds and different fibre contents.

Test speed (mm/min)	Fibre content (wt%)	Tensile strength, σ_t (MPa)
5	0	50.7 (± 1.21)
	10	52.4 (± 1.17)
	20	59.8 (± 1.97)
	30	65.9 (± 1.10)
10	0	53.9 (± 1.15)
	10	55.7 (± 1.23)
	20	60.4 (± 1.19)
	30	67.2 (± 1.42)